



CHORUS

This is the accepted manuscript made available via CHORUS. The article has been published as:

Spontaneous Polarization and Bulk Photovoltaic Effect Driven by Polar Discontinuity in $\text{LaFeO}_3/\text{SrTiO}_3$ Heterojunctions

M. Nakamura, F. Kagawa, T. Tanigaki, H. S. Park, T. Matsuda, D. Shindo, Y. Tokura, and M.
Kawasaki

Phys. Rev. Lett. **116**, 156801 — Published 11 April 2016

DOI: [10.1103/PhysRevLett.116.156801](https://doi.org/10.1103/PhysRevLett.116.156801)

Spontaneous polarization and bulk photovoltaic effect driven by polar discontinuity in $\text{LaFeO}_3/\text{SrTiO}_3$ heterojunctions

M. Nakamura,^{1,*} F. Kagawa,¹ T. Tanigaki,^{1,†} H. S. Park,^{1,‡}

T. Matsuda,² D. Shindo,^{1,3} Y. Tokura,^{1,4} and M. Kawasaki^{1,4}

¹*RIKEN Center for Emergent Matter Science (CEMS), Wako, 351-0198, Japan*

²*Japan Science and Technology Agency (JST), Kawaguchi, 332-0012, Japan*

³*Institute of Multidisciplinary Research for Advanced Materials,
Tohoku University, Sendai 980-8577, Japan*

⁴*Department of Applied Physics and Quantum Phase Electronics Center (QPEC),
University of Tokyo, Tokyo 113-8656, Japan*

(Dated: March 7, 2016)

Abstract

Structurally coherent and chemically abrupt interfaces formed between polar and nonpolar perovskite oxides provide an ideal platform for examining the purely electronic reconstruction known as the polar catastrophe and the emergence of mobile/bound charges at the interface. The appearance of mobile charges induced by the polar catastrophe has already been established in the $\text{LaAlO}_3/\text{SrTiO}_3$ heterojunctions. Although not experimentally verified, the polar catastrophe can also lead to the emergence of spontaneous polarization. We report that thin films of originally nonpolar LaFeO_3 grown on SrTiO_3 are converted into polar as a consequence of the polar catastrophe. The induced spontaneous polarization evokes photovoltaic properties distinct from conventional p - n junctions, such as a switching of photocurrent direction by changing the interfacial atomic sequence. The control of the bulk polarization by engineering the interface demonstrated here will expand the possibilities for designing and realizing new polar materials with photovoltaic functions.

The emergence of mobile and/or bound charges at the interface with discontinuous valence state, or so-called polar discontinuity, has been one of the central research topics in the recent material science [1–4]. The idea of the charge generation stemming from the polar discontinuity had been firstly examined in semiconductor heterojunctions such as Ge/GaAs(110) [5]. However, the atomic interdiffusion is more favored than the purely electronic reconstruction, and the idea had not been verified in these junctions. The revival of the interest on the polar interface was brought by the discovery of the high-mobility two-dimensional (2D) interface conduction in the $\text{LaAlO}_3/\text{SrTiO}_3$ (LAO/STO) heterojunction [1]. Because of the structural robustness and the small atomic diffusibility in the perovskite oxides, their interface can be kept abrupt even in the polar junction. Therefore such interfaces offer an ideal platform to see pure electronic reconstructions and accompanying phenomena distinct from the conventional semiconductor interfaces such as superconductivity [6] and magnetism [7].

The emergence of the 2D conduction in the LAO/STO junction is generally explained by the so-called polar catastrophe scenario as follows [8, 9]. Due to the presence of the polar discontinuity at the interface, high density bound charges ($0.5e/1$ unit cell, corresponding to $53 \mu\text{C}/\text{cm}^2$) should exist at the interface [9, 10]. Because these bound charges evoke the linear divergence of the electrostatic potential with the increasing LAO thickness, the junction reduces the energy cost above certain critical thickness by either collecting electrons to the interface through charge transfer [8] or creating oxygen vacancies and/or other defects on the LAO surface [11–13]. Since the polar catastrophe is a process of charge redistribution necessary to screen the interfacial bound charges, the polar catastrophe can also lead to the displacement of ions or electronic wave functions, thus creating the spontaneous electric polarization, even without collecting mobile charges. Although the emergence of the spontaneous polarization has been theoretically predicted [14, 15], its influence on the junction property is masked by the existence of the mobile charges and therefore is hard to be detected in LAO/STO junction.

Here we explore oxide heterojunctions in which the spontaneous polarization plays a dominant role in the charge screening. The target materials are trivalent transition-metal-oxide insulators which do not form a conductive interface with STO even though the interface has the polar discontinuity [16]. Among them, LaFeO_3 (LFO) is one of the most suitable materials, which is known as a centrosymmetric Mott insulator with an optical gap (2.2 eV) in visible-light region [17]. It has a high resistivity compared to other Mott insulators due

to the closed-shell structure in the up-spin band of Fe^{3+} state [18]. Furthermore, it shows an instability toward polar state under epitaxial strain [19]. Thus, the LFO/STO junction lends itself as a attractive model system to examine the interface-induced spontaneous polarization.

We deposited 30 nm-thick LFO films on 0.5 mm-thick STO and $\text{SrTi}_{0.9998}\text{Nb}_{0.0002}\text{O}_3$ (Nb:STO) substrates with controlled TiO_2 and SrO terminations as illustrated in Fig. 1(a) [20]. Figure 1(b) shows atomic structure and elemental distributions near the LFO/STO interfaces imaged by a scanning transmission electron microscope (STEM) and energy dispersive x-ray spectroscopy (EDX). The image verifies that the elemental sequence is constructed as we designed. The broadening of the distribution estimated from the line profiles of the STEM-EDX intensities remains at most 2 u.c. from the interface [20], indicating that the interface is abrupt enough to classify the interfacial atomic sequence into the two definite types and the effect of the interfacial disorder is negligible. Hereafter, we denote the junctions formed on TiO_2 - and SrO-terminated STO surface as “ TiO_2 junction” and “ FeO_2 junction” according to the interfacial transition-metal layer, respectively. We confirmed that there is no detectable lateral conductivity in those LFO/STO junctions irrespective of the interface terminations.

Current density (J)-voltage (V) characteristics of the junctions measured under photoillumination are shown in Fig. 1(c). Here we shined a laser light with a wavelength of 473 nm ($\hbar\omega = 2.6$ eV), which is absorbed only by LFO. The most prominent feature is that the sign of both the short-circuit photocurrent and the rectifying polarity is reversed by altering the interface termination. Similar switching behavior in the photovoltaic properties has been reported upon ferroelectric polarization reversals in many ferroelectrics [28–30]. Following this analogy, we expect that our LFO films have electric polarization, whose direction is inverted upon altering the interfacial atomic sequence. As discussed later, the polarization direction is fixed by the interfacial atomic sequence and cannot be reversed by electric fields.

To directly see the existence of the electric polarization, we employed piezo-response force microscopy (PFM) to study a sample which is fabricated so that it has both TiO_2 and FeO_2 junctions within the same substrate as shown in Fig. 2(a) [20]. Thus the opposite polarization directions between the two junctions can be clearly visualized within one experimental run. The phase image of PFM shown in Fig. 2(b) exhibits a clear contrast at the boundary with a phase shift of nearly 180 degrees, indicating that the LFO films have electric polarization

components pointing normal to the film surface and their directions are opposite between the two regions. Although this provides a clear evidence for the presence of the electric polarization (P), it still remains unclear whether the polarization is induced by the dielectric response (P_d), or a spontaneous polarization (P_s) existing even without the internal electric field.

The electron holography can directly quantify the spatial distribution of the electrostatic potential and accordingly the built-in internal electric field in a specimen [20]. By employing this technique, we examined the possible origin of P . Figure 3(a) shows the mappings of electrostatic potentials for an electron, which are derived from the phase shift of the object waves. The electrostatic potential is almost uniform in the in-plane direction in both junctions. We now examine in details the electrostatic potential and show in Fig. 3(b) two examples of electrostatic potential obtained along dashed lines in Fig. 3(a). Firstly, the large potential drop near the interface is merely due to the difference in the mean inner potential between LFO and STO and we can thus ignore it in the following discussions. Secondly, the electrostatic potential has opposite slopes in two LFO junctions. The electron potential in LFO grows (falls) from the interface to the surface in TiO_2 (FeO_2) junction with an electric field E of -58 kV/cm ($+81$ kV/cm) as illustrated in Fig. 3(c), **where positive E corresponds to the field pointing from the surface to the bottom of LFO following the definition of the current direction.** The direction of E is consistent with the expected sign of the interface bound charge [31], Thirdly, no appreciable potential variation can be seen in STO, being consistent with no detectable lateral conductivity in the LFO/STO junction. This is in contrast to the downward bending in the case of TiO_2 -terminated LAO/STO that accumulates electrons.

Having clarified the magnitude of the built-in electric field, we now analyze the electrostatic conditions in LFO/Nb:STO junctions. The polar discontinuity entails bound charge of $+0.5e/1$ unit cell ($53 \mu\text{Ccm}^{-2}$) denoted as σ_0 in Fig. 3(d). **We assume that the screening of σ_0 is realized only by the induced polarization (P) in LFO. Then, the potential slope or the built-in electric field (E) observed by electron holography originates from the interfacial remnant charge ($\sigma_0 - P$) given by**

$$\sigma_0 - P = \varepsilon_0 E, \quad (1)$$

where ε_0 is the vacuum permittivity. P is the sum of the dielectric polarization (P_d) and

spontaneous one (P_s), *i.e.*, $P = P_d + P_s$, and P_d is given by

$$P_d = \chi E = \varepsilon_0 \varepsilon_r E, \quad (2)$$

where ε_r stands for the relative dielectric constant of LFO which is derived to be 35 from a capacitance measurement [20]. Using $E = -58$ kV/cm in the TiO₂ junction, we obtain $P_d = 0.17$ $\mu\text{C}/\text{cm}^2$. This value of P_d is far smaller than σ_0 , implying that a large part of the screening charge relies on P_s in our model. Note that, in reality, a part of the screening charge is supplied from the mobile carriers in Nb:STO as revealed by the capacitance measurements [20]. However, both the sign reversal in the polarity of the photovoltaic property and the phase shift of 180° in the PFM observation indicate that a large part of the screening charge comes from P induced in the LFO films.

The existence of the large P_s deduced from above analysis is justified by the anomalous photovoltaic properties. The direction of photocurrent should have been aligned to the electric field in conventional dielectrics. However, the experimentally observed short-circuit photocurrent (Fig. 1(c)) flows opposite to the direction of the built-in electric field (Fig. 4(a)), and also opposite to that reported for LAO/STO junction where the spontaneous polarization is negligibly small after mobile carriers are induced by the polar catastrophe [32]. This means that the photocurrent in our junctions originates from a different mechanism, likely being associated with the P_s . Here we introduce a concept of the shift current (J_{shift}) as a possible origin of the photocurrent in our junctions. It is known that single-domain noncentrosymmetric materials can generate DC current under uniform photoillumination, namely the bulk photovoltaic effect [33]. A main origin of the bulk photovoltaic effect which has been recently proven to be is the shift current [34–36]. The shift current arises from the quantum mechanical displacement of the photo-induced carriers relative to the initial state in real space due to the asymmetric electronic potential in inversion-broken materials as depicted in Fig. 4(a). The shift current flows to the direction of the so-called shift vector given by the difference in the Berry connections between the initial and excited states [35, 36]. Therefore, the shift current direction depends strongly on the relevant band structure rather than the macroscopic electric field. We consider that the shift current and drift current (J_{drift}) are coexisting in our junctions, and the shift current is the origin of the photocurrent flowing opposite to E .

The coexistence of the J_{shift} and the J_{drift} is evidenced in the spectral distribution of

the short-circuit photocurrent (J_{SC}), so-called photocurrent action spectra. As shown in Fig. 4(b), the sign of J_{SC} reverses in TiO_2 junction with a LFO thickness of 20 nm, from negative to positive at the photon energy of 3.2 eV. The negative (positive) J_{SC} indicates a dominating J_{drift} (J_{shift}). The sign change occurs because of the enlargement of J_{shift} at higher photon energies. Such a sign reversal is not observed in the junctions with $t = 13$ nm and 30 nm in the entire photon energy range, but these two junctions have opposite J_{SC} : in the former (latter), the sign is negative (positive). We examined the position dependence of photocurrent action spectra in an array of devices [20]. The spectra are reproducible and independent of the device position, implying that the anomalous sign change in the photocurrent is not induced by local defects [25].

Now we discuss an evolution of the polarization and according change in the photocurrent with a thickness on the basis of the polar catastrophe model. There are two characteristic thicknesses, t_c and t'_c . t_c is the thickness at which the polar catastrophe sets on and t'_c is the thickness at which J_{SC} reverses the sign. We consider the mechanisms of the photocurrent generation in the following three thickness ranges; (i) $t < t_c$, (ii) $t_c \leq t < t'_c$, and (iii) $t'_c \leq t$, as shown in Fig. 4(c). In case (i), the spontaneous polarization is absent ($P_s = 0$) and the most of σ_0 is screened by the dielectric response associated with the large thickness-independent E . Equations (1) and (2) give $E = \sigma_0/\varepsilon_0(1 + \varepsilon_r)$, and E is estimated to be -17 MV/cm in LFO. Due to the large E , J_{drift} is dominant in this thickness range, resulting in the same direction between E and J_{SC} . When the potential elevation (ϕ) reaches the band gap of LFO ($\Delta=2.2$ eV), the polar catastrophe occurs and triggers the emergence of P_s . We define this thickness as t_c , given by $\varepsilon_0(1 + \varepsilon_r)\Delta/\sigma_0$, which is estimated to be 1.4 nm (~ 3 u.c.) in LFO/STO junction. For $t > t_c$, E decreases in inversely proportion to t because ϕ is limited by Δ . In contrast, P_s grows with t to compensate for the reduced dielectric response. Since $J_{\text{drift}} \propto E$ and J_{shift} has a positive correlation with P_s , J_{drift} (J_{shift}) decreases (increases) with t , implying that J_{drift} and J_{shift} crosses at some thickness, which we define as t'_c . In case (ii), J_{drift} is still larger than J_{shift} and hence J_{SC} and E points to the same direction, which is the case for the junction with $t = 13$ nm. In case (iii), J_{shift} overcomes J_{drift} and hence J_{SC} flows opposite to E as observed for the junction with $t = 32$ nm. Hence, the junction with $t = 20$ nm will be located very close to the critical thickness t'_c .

Figure 4(d) shows the dependence of P_s and P_d on t calculated on the basis of the polar catastrophe model. The curves are plotted for $\phi = 2.2$ eV and 0.17 eV which are

the upper limit estimated from the band gap of LFO and the lower limit estimated from the electron holography, respectively. Figure 4(e) shows the thickness dependence of the photocurrent at 2.8 eV and 3.5 eV obtained from the action spectra. The sign is negative in thinner junctions due to the dominant J_{drift} and switches to positive in thicker junctions driven by the enhanced J_{shift} . The sign reversal occurs between 17 and 25 nm depending on the photon energy, implying that t'_c locates in this thickness range. The photocurrent of the thickest film of nearly 70 nm is quite small. This is probably because the typical length of the shift vector is 10-100 nm and the photocurrent reduces when the film thickness exceeds this length [37]. Thus, the model calculation of P_s and P_d shown in Fig. 4(d) can qualitatively explain the thickness dependence of the photocurrent, although the relation between J_{shift} and the electric polarization is complicated and the quantitative estimation of J_{shift} is currently impossible.

We again emphasize that the dominant screening mechanism of the polar discontinuity in LFO/STO junction is the spontaneous polarization, unlike the mobile charges in LAO/STO. The reason for the difference between LFO/STO and LAO/STO junctions can be following. According to a first-principles calculation, $R\text{FeO}_3$ (R stand for rare-earth elements) can show a spontaneous polarization over $100 \mu\text{C}/\text{cm}^2$ if 7 % of compressive strain is applied [19]. Because the strain in our LFO film is only 1 %, the epitaxial strain alone is unlikely to be sufficient story in order to induce the polar state. Yet, the instability towards polar state in LFO will assist the emergence of the spontaneous polarization.

In summary, we have revealed the emergence of spontaneous polarization in $\text{LaFeO}_3/\text{SrTiO}_3$ heterojunctions. The existence of the electric polarization was verified by piezo-response force microscopy. Furthermore, electron holography has revealed that the spontaneous polarization dominates the electric polarization. The polarization direction can be switched by the choice of interfacial atomic sequence. The emergent spontaneous polarization induces anomalous photovoltaic properties in the junctions, such as a sign reversal in the photocurrent depending on the interfacial atomic sequence and the excitation photon energy. The present demonstration implies that the control of the bulk polarization can be achieved by engineering the interface. Recently visible-light-absorbable polar oxides have been widely explored and suggested to be efficient photovoltaic materials [38–40]. Our present results offer a feasible way of realizing new photovoltaic materials from narrow-gap and non-polar ones by engineering the heterointerfaces of oxides.

We appreciate H. Y. Hwang, A. Tsukazaki, N. Ogawa, and D. Maryenko for useful discussions and Y. Ohtsu and T. Sato for TEM observation. This work was partly supported by the Japan Society for the promotion of Science (JSPS) through its Funding Program for World-Leading Innovative R&D on Science and Technology (FIRST Program), Grant-in-Aid for Young Scientists (A) (15H05426) and that for Scientific Research (24226002) from the MEXT of Japan, and CREST from Japan Science and Technology Agency (JST).

* Electronic address: `masao.nakamura@riken.jp`

† Present address: Research and Development Group, Hitachi, Ltd., Hatoyama, Saitama 350-0395, Japan

‡ Present address: Department of Materials Science and Engineering, Dong-A University, Busan 604-714, Republic of Korea

- [1] A. Ohtomo and H. Y. Hwang, *Nature (London)* **427**, 423 (2004)
- [2] J. Mannhart and D. G. Schlom, *Science* **327**, 1607 (2010).
- [3] R. Pentcheva, W. E. Pickett, *J. Phys.: Condens. Matter* **22**, 043001 (2010).
- [4] H. Y. Hwang, Y. Iwasa, M. Kawasaki, B. Keimer, N. Nagaosa, and Y. Tokura, *Nat. Mater.* **11**, 103 (2012).
- [5] W. A. Harrison, E. A. Kraut, J. R. Waldrop, and R. W. Grant, *Phys. Rev. B* **18**, 4402 (1978).
- [6] N. Reyren *et al.*, *Science* **317**, 1196 (2007).
- [7] A. Brinkman *et al.*, *Nat. Mater.* **6**, 493 (2007).
- [8] N. Nakagawa, H. Y. Hwang, and D. A. Muller, *Nat. Mater.* **5**, 204 (2006).
- [9] N. C. Bristowe, P. Ghosez, P. B. Littlewood, and E. Artacho, *J. Phys.: Condens. Matter* **26**, 143201 (2014).
- [10] M. Stengel and D. Vanderbilt, *Phys. Rev. B* **80**, 241103 (2009).
- [11] C. Cen *et al.*, *Nat. Mater.* **7**, 298 (2008).
- [12] Y. Li, S. N. Phattalung, S. Limpijumnong, J. Kim, and J. Yu, *Phys. Rev. B* **84**, 245307 (2011).
- [13] L. Yu and A. Zunger, *Nat. Commun.* **5**, 5118 (2014).
- [14] N. C. Bristowe, E. Artacho, and P. B. Littlewood, *Phys. Rev. B* **80**, 045425 (2009).
- [15] R. Pentcheva and W. E. Pickett, *Phys. Rev. Lett.* **102**, 107602 (2009).
- [16] S. A. Chambers, L. Qiao, T. C. Droubay, T. C. Kaspar, B. W. Arey, and P. V. Sushko, *Phys.*

- Rev. Lett. **107** 206802 (2011).
- [17] M. Imada, A. Fujimori, and Y. Tokura, Rev. Mod. Phys. **70**, 1039 (1998).
- [18] T. Arima, Y. Tokura, and J. B. Torrance, Phys. Rev. B **48**, 17006 (1993).
- [19] H. J. Zhao, Y. Yang, W. Ren, A.-J. Mao, X. M. Chen, and L. Bellaiche, J. Phys.: Condens. Matter **26**, 472201 (2014).
- [20] See Supplemental Material. It cites Refs. [21-27].
- [21] M. Kawasaki *et al.*, Science **266**, 1540 (1994).
- [22] G. Kothleitner, M. J. Neish, N. R. Lugg, S. D. Findlay, W. Grogger, F. Hofer, and L. J. Allen, Phys. Rev. Lett. **112**, 085501 (2014).
- [23] M. Nakamura, A. Sawa, J. Fujioka, M. Kawasaki, and Y. Tokura, Phys. Rev. B **82**, 201101(R) (2010).
- [24] T. Tanigaki, Y. Inada, S. Aizawa, T. Suzuki, H. S. Park, T. Matsuda, A. Taniyama, D. Shindo, and A. Tonomura, Appl. Phys. Lett. **101**, 043101 (2012).
- [25] L. Pintilie, V. Stancu, E. Vasile, and I. Pintili, J. Appl. Phys. **107**, 114111 (2010).
- [26] W. Siemons, G. Koster, H. Yamamoto, W. A. Harrison, G. Lucovsky, T. H. Geballe, D. H. A. Blank, and M. R. Beasley, Phys. Rev. Lett. **98**, 196802 (2007).
- [27] G. Herranz, M. Basletić, M. Bibes, C. Carrétéro, E. Tafra, E. Jacquet, K. Bouzouane, C. Deranlot, A. Hamzić, J.-M. Broto, A. Barthélémy, and A. Fert, Phys. Rev. Lett. **98**, 216803 (2007).
- [28] T. Choi, S. Lee, Y. J. Choi, V. Kiryukhin, and S.-W. Cheong, Science **324**, 63 (2009).
- [29] C. J. Won, Y. A. Park, K. D. Lee, H. Y. Ryu, and N. Hur, J. Appl. Phys. **109**, 084108 (2011).
- [30] Y. Yuan, T. J. Reece, P. Sharma, S. Poddar, S. Ducharme, A. Gruverman, Y. Yang, and J. Huang, Nat. Mater. **10**, 296 (2011).
- [31] G. Singh-Bhalla *et al.*, Nat. Phys. **7**, 80 (2011).
- [32] H. Liang *et al.*, Sci. Rep. **3**, 1975 (2013).
- [33] B. I. Sturman, and V. M. Fridkin, *The photovoltaic and photorefractive effects in noncentrosymmetric materials*. (Goldon and Breach Science Publishers, 1992).
- [34] R. von Baltz and W. Kraut, Phys. Rev. B **23**, 5590 (1981).
- [35] S. M. Young and A. M. Rappe, Phys. Rev. Lett. **109**, 116601 (2012).
- [36] T. Moritomo and N. Nagaosa, arXiv:1510.08112 (2015).
- [37] A. Zenkevich, Yu. Matveyev, K. Maksimova, R. Gaynutdinov, A. Tolstikhina, and V. Fridkin,

- Phys. Rev. B **90**, 161409(R) (2014).
- [38] S. Y. Yang *et al.*, Appl. Phys. Lett. **95**, 062909 (2009).
- [39] I. Grinberg *et al.* Nature (London) **53**, 509 (2013).
- [40] R. Nechache, C. Harnagea, S. Li, L. Cardenas, W. Huang, J. Chakrabartty, and F. Rosei, Nat. Photonics **9**, 61 (2015).

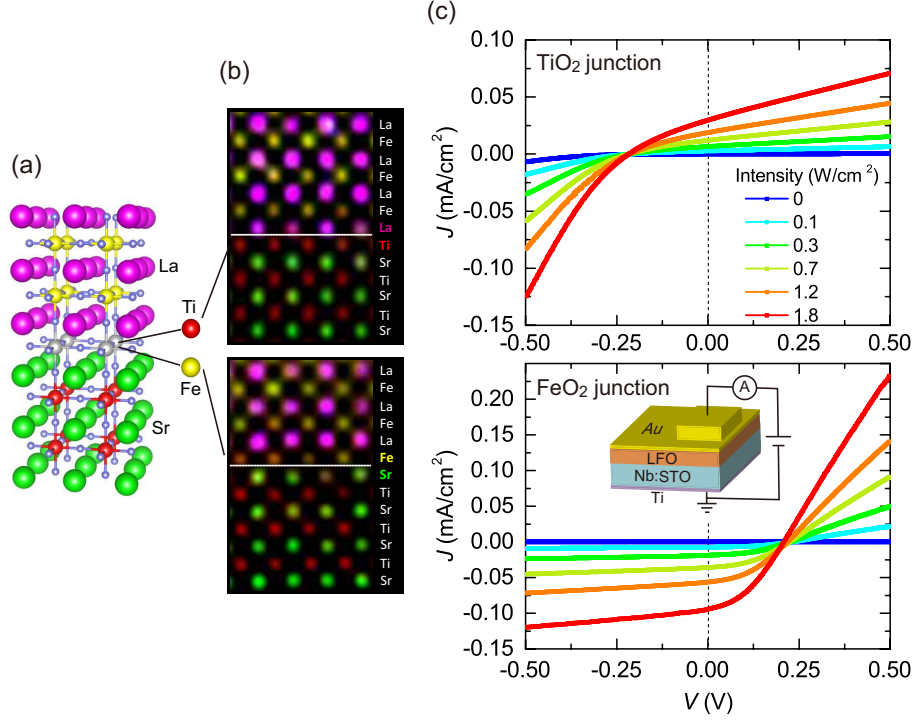


FIG. 1: (Color online) (a) A schematic of the elemental stacking in LFO/STO junctions. The interfacial atomic layers were controlled either TiO₂ or FeO₂ layers. (b) Elemental distribution mappings for a TiO₂ junction (upper panel) and FeO₂ junction (lower panel) taken with a scanning transmission electron microscope (STEM), where atomic resolution energy-dispersive x-ray spectroscopy (EDX) images are superimposed on high-angle annular dark (HAADF) images. Line profiles of the elemental distribution are shown in the Supplementary Materials [20]. (c) Current density (J)-voltage (V) properties of LFO/Nb:STO junctions with shining a laser light. The wavelength of the laser is 473 nm. The positive direction of the applied voltage is defined as the schematics illustrated in inset.

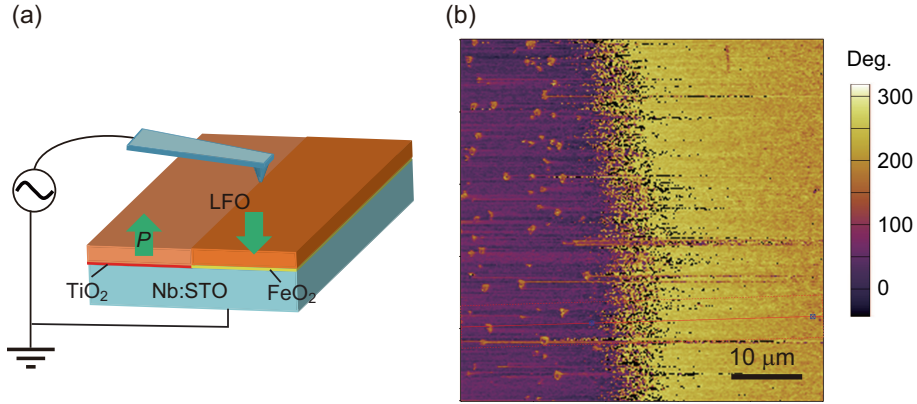


FIG. 2: (Color online) (a) A schematic of piezoresponce force microscope (PFM) observation for a LFO film grown on a Nb doped STO substrate having both TiO_2 and SrO surface terminated regions on the surface. (b) Observation of artificially tailored polarization domains by PFM as a phase image. The boundary of the opposite polarization domains is coincident with that of the interface termination.

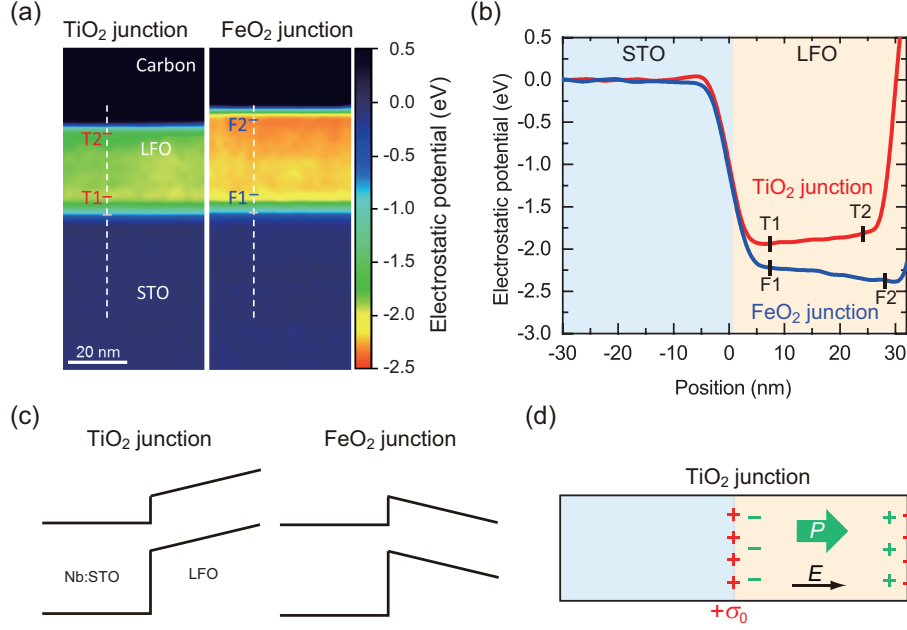


FIG. 3: (a) Mappings of electrostatic potentials derived from electron holography for two differently interfaced LFO/STO junctions. Here we show the potentials for an electron. (b) Line profiles of the potentials along the dashed lines in Fig. 3(a). (c) Possible band structure in the LFO/STO junctions deduced from the potential profiles in Fig. 3(b) and capacitance measurements [20]. (d) A model for electrostatic conditions in a TiO_2 junction. σ_0 denotes bound charges stemming from the polar discontinuity between LFO and STO. P is an electric polarization induced in LFO to partially screen σ_0 . E is a built-in electric field originated from the remnant interface charges ($\sigma_0 - P$).

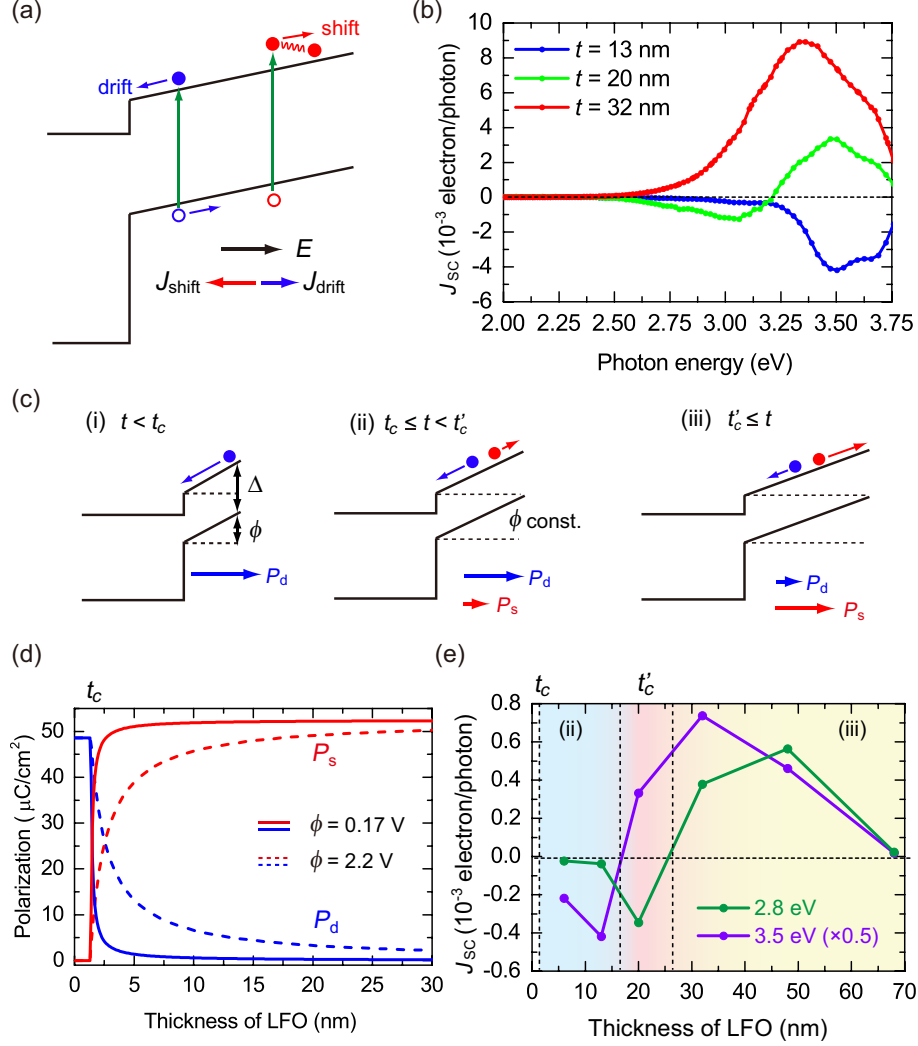


FIG. 4: (Color online) (a) Schematic of two possible origins of photocurrent in LFO/STO junction. The shift current (J_{shift}) is induced by the spontaneous polarization while the drift current (J_{drift}) is induced by the internal electric field. (b) Photocurrent action spectra for TiO₂ junctions with different LFO thicknesses. (c) Band structures and photocurrent generation in LFO/STO junctions in three thickness ranges. Δ and ϕ stand for the band gap of LFO and the potential elevation, respectively. Case (i): The slope of the electrostatic potential is constant and the origin of the photocurrent is J_{drift} only. Case (ii): When $t > t_c$, ϕ is constant and J_{drift} and J_{shift} coexist. Case (iii): At $t = t'_c > t_c$, J_{shift} becomes more dominant than J_{drift} . (d) Calculated thickness dependence of the spontaneous polarization (P_s) and dielectric polarization (P_d) on the basis of the band structure. Solid (dashed) lines correspond to the case of $\phi = 0.17$ eV (2.2 eV). (e) Magnitude of the photocurrent as a function of the thickness of LFO in TiO₂ junctions measured at 2.8 and 3.5 eV.